MDPI

Combined Adsorption and Photocatalytic Degradation for Ciprofloxacin Removal Using Sugarcane Bagasse/N,S-TiO$_2$ Powder Composite

Linh Thuy Nguyen [1,2], Hanh Thi Nguyen [2], Khai Manh Nguyen [2], Thuy Thi Pham [2] and Bart Van der Bruggen [1,*]

[1] Laboratory for Process Engineering for Sustainable Systems, Department of Chemical Engineering, KU Leuven, Celestijnenlaan 200F, 3001 Leuven, Belgium; thuylinh_mt@hus.edu.vn

[2] Faculty of Environmental Sciences, University of Science, Vietnam National University, 334 Nguyen Trai, Thanh Xuan, Hanoi 700000, Vietnam; hanhnguyen@hus.edu.vn (H.T.N.); nguyenmanhkhai@hus.edu.vn (K.M.N.); phamthithuy@hus.edu.vn (T.T.P.)

* Correspondence: bart.vanderbruggen@kuleuven.be

Abstract: N,S-TiO$_2$ deposited on three kinds of pre-treated sugarcane bagasse was synthesized via a sol–gel method. The obtained composites were characterized by various techniques, including scanning electron microscopy (SEM), X-ray diffraction (XRD), Fourier-transform infrared spectroscopy (FTIR), and photoluminescence spectroscopy (PL). UV-visible induced degradation of ciprofloxacin was investigated. The influence of some experimental parameters such as contact time, pH, dosage, and initial concentration on the efficiency of ciprofloxacin elimination was also evaluated. The highest efficiency was observed for the alkaline pre-treated sugarcane bagasse combined with N,S-TiO$_2$, about 86% under optimal conditions (contact time 150-min irradiation, pH 5.5–6, dosage 0.5 g L^{-1}, and the initial concentration CIP 30 ppm). There may be a rapid ciprofloxacin transition from the adsorption site to the photocatalytic site, and the alkaline pre-treated sugarcane bagasse/N,S-TiO$_2$ prevented the recombining of holes and electrons of the photocatalyst. Furthermore, the alkaline pretreatment sugarcane bagasse/N,S-TiO$_2$ composite material was sustainable, with only a 10% reduction after reusing the material three times. The presence of sugarcane bagasse made the material easy to recover from the liquid phase.

Keywords: sugarcane bagasse; ciprofloxacin; antibiotic; N,S-TiO$_2$; photocatalyst

1. Introduction

For water purification, various technologies are used, which include conventional techniques (coagulation/flocculation, sedimentation, filtration), adsorption, membrane filtration, and advanced oxidation processes [1]. Conventional techniques and adsorption are frequently applied because of their economy, simple design, and easy application [2]; however, they do leave some harmful organic substances non-decomposed and generate a new waste (solid phase). This drawback is similar to implementing membrane technology because the pollutants are not degraded but transferred to a more concentrated fraction [3]. Advanced oxidation processes, such as Fenton reaction [4], catalytic ozonation [5,6], and photocatalytic oxidation [7], are based on the creation of hydroxyl radicals that can degrade contaminants, especially those that are difficult to biodegrade, and have clearly proved to be a viable method on the industrial scale [8]. Photocatalytic oxidation processes using titanium dioxide (TiO$_2$) are considered the most promising and efficient among the different potential methods due to their well-known properties [9–11]. However, there are two limitations to its practical application: (i) the large bandgap energy (3.2 eV for anatase TiO$_2$) limits its use to UV light; (ii) the high recombination rate of electrons and holes, reported to reach 90% [12,13]. Many studies have shown that doping substances such as metals and non-metals on TiO$_2$ reduce the bandgap energy and expand light absorption

to the visible region; it was reported that non-metallic doping is highly stable and more active than metallic doping [14,15]. Nitrogen, sulfur, and carbon are the most frequently used non-metal dopants due to their visible light response and quantum efficiency of the TiO_2 lattice, enhancing photocatalytic activity [9].

Apart from doping, TiO_2 can also improve the adsorption of photocatalysts by constructing a composite with support materials or by incorporating secondary materials [16]. On the other hand, support materials help to reduce the agglomeration of TiO_2 nanoparticles over time and allow them to overcome difficulties in their recovery from suspension [17]. Various supports have been explored with TiO_2 as zeolites [16], silica [18], clay [14], activated carbon [19], biochar [20,21], kaolin [22], and graphene [23]. Low-cost biomass as carbonaceous source receives significant attention due to its typical large surface area and well-developed porosity. Sugarcane bagasse is a waste residue of the sugar industry [24], having a typical lignocellulosic biomass composed of cellulose (40–45%), hemicellulose (30–35%), and lignin (20–30%) [25]; it has the potential to make part of a composite with TiO_2. This meets the criteria of today's ambition for a circular economy, as it turns waste into an input for another closed production cycle, in contrast to the "take-make-waste" approach.

The occurrence of antibiotics in water sources in many countries is one of the obstacles to achieving the goal of clean water for all. Ciprofloxacin (CIP) belongs to the fluoroquinolones group, which comprises third generation antibiotics. It is very commonly used to give medical care for infectious diseases in humans, pets, livestock, and fish farms [26]. It can spread into the environment through water sanitation systems, cultivated crops, and food chains; they are a potential threat to the ecosystem and community [27]. Concentrations as high as 50 mg L^{-1} have been detected near drug manufacturing plants [28] and from 620–246, 100 ng L^{-1} in the influent and effluent of wastewater treatment plants in North America and Europe [29]. It is also considered as one of the 10 high concentration pharmaceutical substances [26]. Therefore, the removal of CIP from water is an emerging problem of concern.

From that point of view, a novel sugarcane bagasse/N,S-TiO_2 hybrid photocatalyst was studied to overcome the limitations mentioned above. Sugarcane bagasse was chemically activated by alkaline and couple acidic–alkaline agents used for the N,S-TiO_2 composite. Sugarcane bagasse/N,S-TiO_2 was characterized and tested to determine its ciprofloxacin removal abilities in comparison with N,S-TiO_2. The influence of the experimental parameters was evaluated to find the optimal processing conditions and finally, its performance and stability after recycling was also investigated.

2. Experimental Section

2.1. Chemicals

Tetraisopropyl orthotitanate ($C_{12}H_{28}O_4Ti$); thiourea (CH_4N_2S); ethanol 99% (C_2H_5OH); nitric acid 65% (HNO_3); hydrochloric acid (HCl); sodium hydroxide (NaOH); and ciprofloxacin hydrochloride ($C_{17}H_{18}FN_3O_3 \cdot HCl$), all of analytical grade, were purchased from Sigma-Aldrich and were used without further purification.

2.2. Preparation Materials

2.2.1. Pretreatment Sugarcane Bagasse

The obtained sugarcane bagasse from a local market was cut into pieces of 5 cm and washed several times with tap water and hot water and was then dehydrated in an oven at 70 °C until a constant weight was obtained. Dried sugarcane bagasse was ground and sieved to 0.5 cm fractions, denoted as RSB (raw sugarcane bagasse without chemically pre-treatment), which was used for further chemical modification. An appropriate amount, 10 g RSB, was immersed in a solution containing 1.5 mol L^{-1} sodium hydroxide. The materials were washed by deionized water, filtered after 24 h, and dried at 80 °C overnight, becoming ASB (alkaline pretreated sugarcane bagasse). The last adsorbent CSB (two-stage acidic-alkaline pretreated sugarcane bagasse) was obtained by using 10 g RSB having

completely imbibed 1 mol L^{-1} nitric acid, which was then washed, filtered, and dried under the same conditions as ASB followed by soaking in 1.5 mol L^{-1} sodium hydroxide solution. Next, the suspension was filtered, washed with deionized water, and dried at 80 °C until constant weight was reached. RSB, ASB, and CSB were stored and used as supported material in the following experiments.

2.2.2. Synthesis of Sugarcane Bagasse/N,S-TiO$_2$ Composite

The sugarcane bagasse/N,S-TiO$_2$ composite was prepared by a similar method reported in a previous study [30] by adding 3g sugarcane bagasse to the thiourea and nitric acid solution. The samples were denoted as RSB/N,S-TiO$_2$, ASB/N,S-TiO$_2$, and CSB/N,S-TiO$_2$ after calcination at 450 °C in a furnace for 2 h.

2.3. Characterization of Materials

The crystalline phases of the N,S-TiO$_2$ and sugarcane bagasse/N,S-TiO$_2$ composite samples were identified by X-ray diffraction (XRD) using a Rigaku-MiniFlex 600 diffractometer(Rigaku, Tokyo, Japan). The morphology of the samples was revealed by scanning electron microscopy (SEM) using a Jeol–model JEM 1010 microscope, (JEOL Ltd., Tokyo, Japan). The functional groups of samples were explored by Fourier-transform infrared spectroscopy (FTIR) using a Jasco FTIR-4600 spectrometer (Jasco Products Company, Oklahoma, OK, USA). The quenching of photoluminescence spectroscopy (PL) was recorded using a Horiba PL FluoroMax-4 spectrofluorometer (Horiba, Tokyo, Japan).

2.4. Experimental Approach

Experimental design and measurement of antibiotic concentration after the reaction were conducted as described elsewhere [30]. An adequate weight of synthesized sample was added in 100 mL CIP solution until achieving an adsorption–desorption equilibrium (45 min) before exposure UV-vis light from a halogen lamp of 500 W under atmospheric pressure and at room temperature.
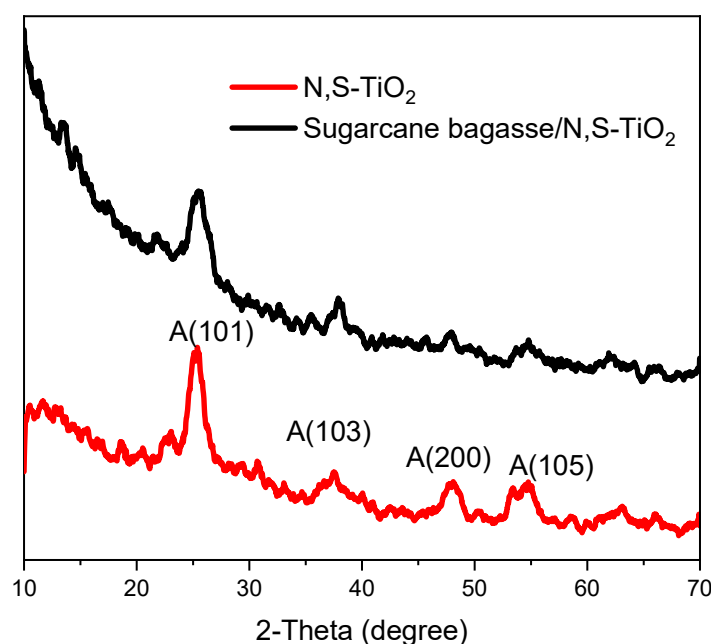
RSB/N,S-TiO$_2$, ASB/N,S-TiO$_2$, and CSB/N,S-TiO$_2$ composite samples were tested to remove CIP in comparison to the synthetic N,S-TiO$_2$ that was prepared using the procedure described in the literature [30]. The effects of pH, dosage, contact time, and the initial concentration on CIP removal were studied. Samples were taken and analyzed with a UV–vis analyzer (Shimadzu, Tokyo, Japan) at a wavelength of 276 nm. The CIP removal efficiency was evaluated through the C_t/C_o ratio, with C_t and C_o representing the equilibrium and initial CIP concentration (ppm), respectively. The stability of the photocatalyst composite was tested three times to assess its reusability.

3. Results
3.1. Characterization of Materials
3.1.1. XRD

In Figure 1, XRD analysis was performed to characterize the nitrogen and sulfur co-doped TiO$_2$ and sugarcane bagasse/N,S-TiO$_2$ composite. Since RSB/N,S-TiO$_2$, ASB/N,S-TiO$_2$, and CSB/N,S-TiO$_2$ have the same XRD spectrum, a general plot called sugarcane bagasse/N,S-TiO$_2$ is shown. The peaks at the 2-Theta angles correspond to the (101), (103), (200), and (105) diffraction planes of the anatase phase [30]. The pre-treatments of the sugarcane bagasse did not change the crystal structure of the photocatalyst. With a 100% anatase structure, the composite material exhibits a better photocatalytic degradation than the rutile or brookite phase [31].

**Figure 1.** XRD spectrum of N,S-TiO$_2$ and sugarcane bagasse/N,S-TiO$_2$ composite.

3.1.2. SEM

SEM images of N,S-TiO$_2$, RSB/N,S-TiO$_2$, ASB/N,S-TiO$_2$, and CSB/N,S-TiO$_2$ are shown in Figure 2. N,S-TiO$_2$ nanoparticles have a uniform, even, smooth surface and a spherical shape. Composite materials have a different surface morphology; specifically, RSB/N,S-TiO$_2$ has a rough and uneven surface compared to ASB/N,S-TiO$_2$ and CSB/N,S-TiO$_2$; ASB/N,S-TiO$_2$ seems to be more abrasive than RSB/N,S-TiO$_2$; therefore, it is smoother and more uniform. CSB/N,S-TiO$_2$ is in the form of the corroded plates. ASB/N,S-TiO$_2$ material has a smoother surface; therefore, the N,S-TiO$_2$ nanoparticles can be easily exposed to light to generate the reactive oxygen species that are necessary for antibiotic degradation reaction. In contrast, RSB/N,S-TiO$_2$ and CSB/N,S-TiO$_2$ have catalyst particles located deep inside, making it difficult for N,S-TiO$_2$ particles to be exposed to light.

3.1.3. FT-IR

FT-IR results are shown in Figure 3. Spectra were used to identify the surface functional groups of composite synthesized samples. Broad peaks within the 400–800 cm^{-1} range are related to Ti-O, Ti-O-Ti, O-Ti-O, and Ti-O-C bonds [32,33]. The low FT-IR frequencies of RSB/N,S-TiO$_2$ and CSB/N,S-TiO$_2$ in this range may be because of the low titanium and oxygen element concentration. Ti-O-N and Ti-O-S bonds appear at the bands between 1047–1055 cm^{-1} and 1130–1441 cm^{-1}, respectively [33,34], which clearly show in the co-doped composites of N,S-TiO$_2$ and ASB/N,S-TiO$_2$. The bands in the regions 1500–1600 cm^{-1} and 2800–2900 cm^{-1} are attributed to the stretching of the C–O–O groups, the symmetric vibration of C–H, and asymmetric vibration of C–H [20]. The peak around 1630–1640 cm^{-1} is assigned to the bending vibrations of either O-H or the stretching vibration N-H [32,35]. According to Mohamed et al. (2019), the Ti-N-O-C bonds can be formed at the peak of 1700 cm^{-1} [32]. The peak at 3300–3500 cm^{-1} corresponds to the O-H stretching and bending vibrations of the hydroxyl groups and the adsorbed water molecules [33]. The presence of the elements N, S, Ti is confirmed in the three material composites through the FTIR results.

(a)

(b)

(c)

(d)
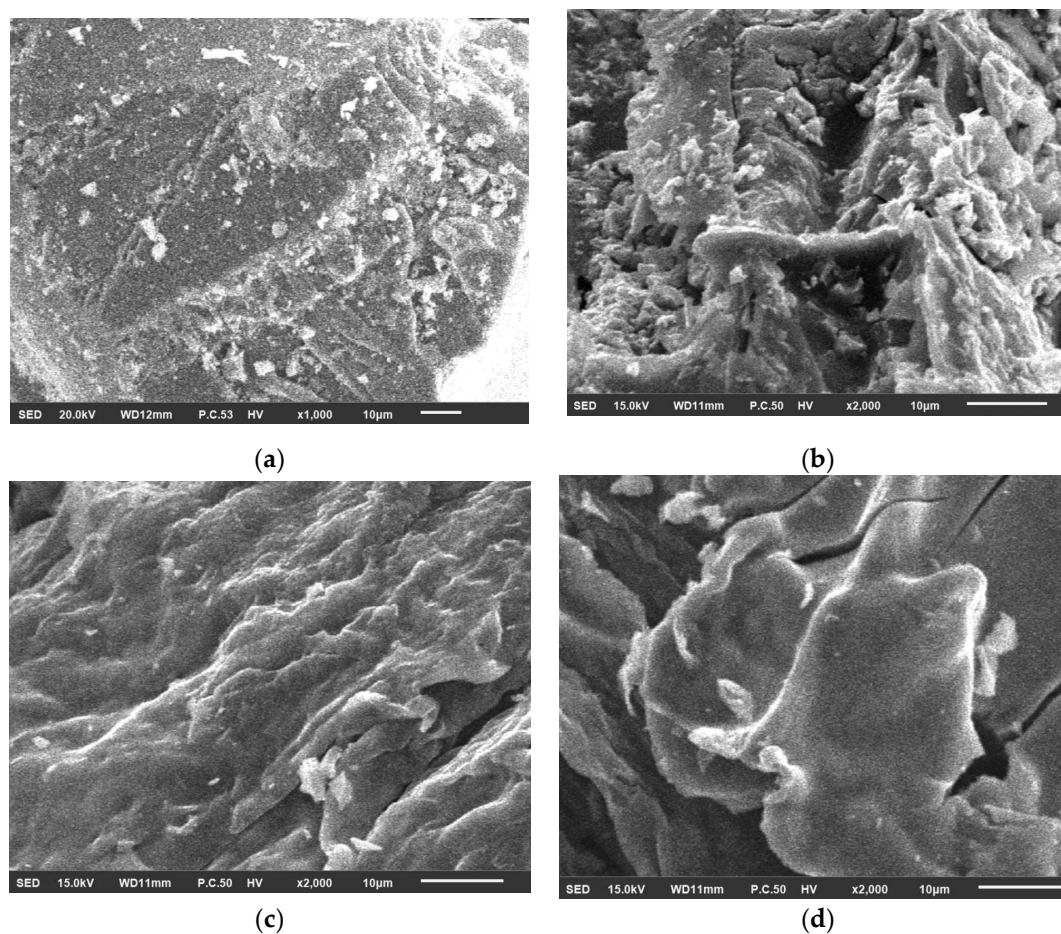
Figure 2. Morphology of N,S-TiO$_2$ (**a**), RSB/N,S-TiO$_2$ (**b**), ASB/N,S-TiO$_2$ (**c**), and CSB/N,S-TiO$_2$ (**d**).
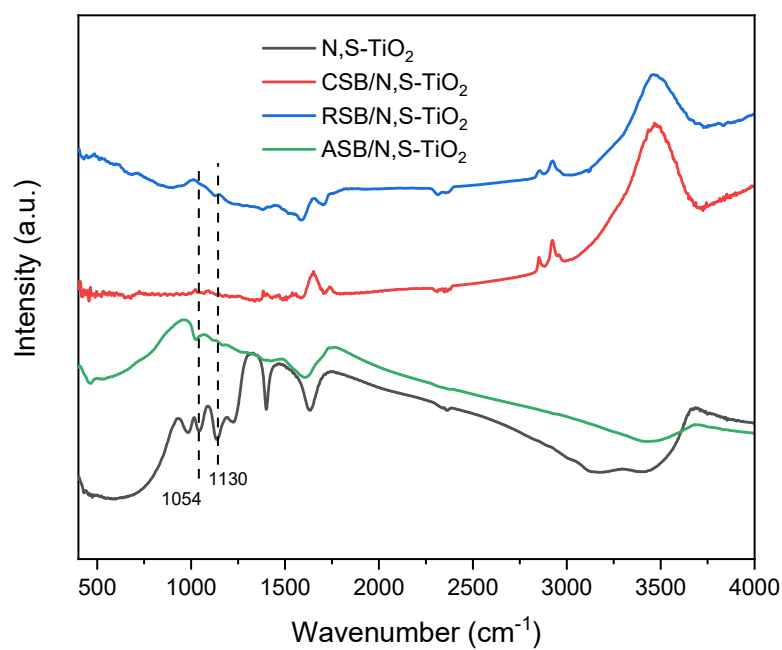
Figure 3. FTIR spectra for N,S-TiO$_2$; RSB/N,S-TiO$_2$; ASB/N,S-TiO$_2$; and CSB/N,S-TiO$_2$ composite photocatalysts.

3.1.4. Photoluminescence

Photoluminescence spectra were used to investigate the recombination of electron–hole pairs in the composite materials compared to N,S-TiO$_2$. This is shown Figure 4. It can be seen that the photoluminescence intensity of CSB/N,S-TiO$_2$ is the highest compared to other materials and decreases steadily in RSB/N,S-TiO$_2$; N,S-TiO$_2$; and ASB/N,S-TiO$_2$. ASB/N,S-TiO$_2$ can be predicted to have better photocatalytic activity since the recombination of the e$^-$/h pairs is minimal. After calcination at 450 °C, sugarcane bagasse naturally converted into biochar, which can trap electrons at conduction band energy. The alkaline pre-treated sugarcane bagasse may strengthen the activated state of the photocatalyst since the vacant d orbitals of metals present in biochar act as electron acceptors that prevent the recombination of the e$^-$/h pairs; therefore, the production of OH$^\bullet$, H$_2$O$_2$, and O$_2^{\bullet-}$ when in contact with O$_2$ on the surface of the material [36] causes an improvement in the photocatalytic degradation. The results also suggest that the pretreatment methods of support material influence the photocatalytic material properties.
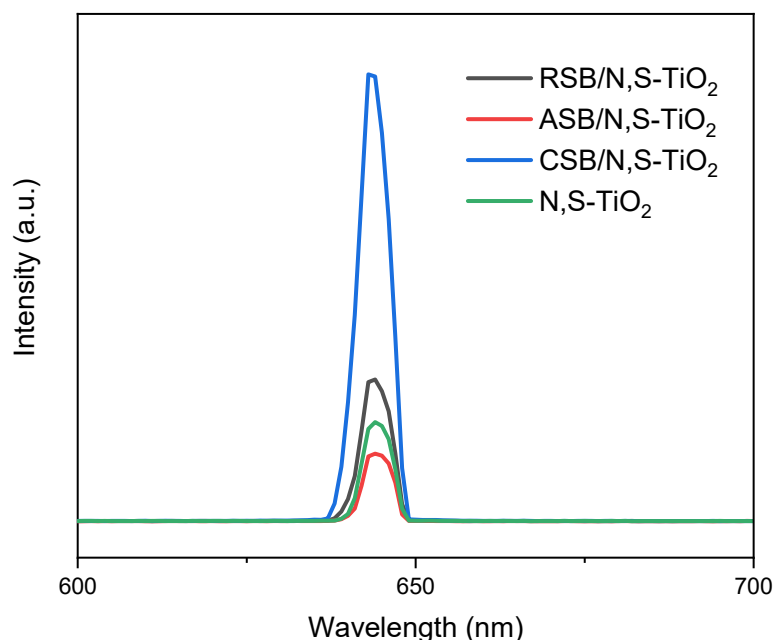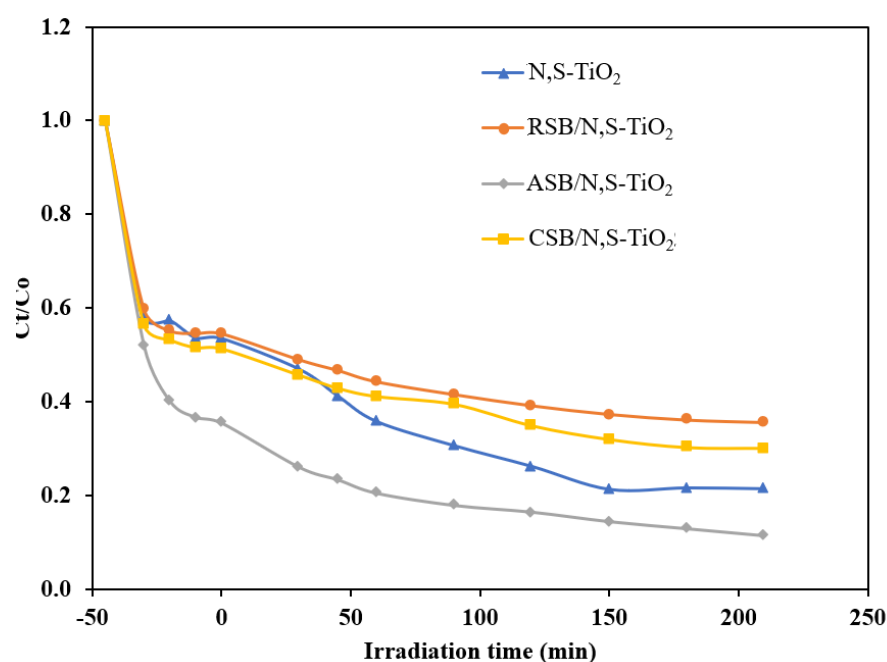

Figure 4. Photoluminescence of N,S-TiO$_2$ and three composite materials.

3.2. Elimination of CIP

#### 3.2.1. Adsorption Reaction and Photocatalytic Degradation

Figure 5 shows the adsorption reaction and photocatalytic degradation of CIP of nitrogen, sulfur co-doped TiO$_2$, and three composite materials. It was observed that about 46–49% CIP in solution absorbed on N,S-TiO$_2$; RSB/N,S-TiO$_2$; and CSB/N,S-TiO$_2$ after 45 min in the dark, while the amount of CIP removed by ASB/N,S-TiO$_2$ was approximately 66%. This suggests that N,S-TiO$_2$ incorporation with alkaline pre-treated sugarcane bagasse improved the antibiotic adsorption capacity. CIP concentrations tended to decrease sharply during about 60 min of illumination; after that, they gradually decreased in all four materials. The alkaline pretreated sugarcane bagasse gave the highest antibiotic treatment efficiency compared to the non-pretreated and acid–base pretreatment samples. ASB/N,S-TiO$_2$ was chosen for the effect of the experimental parameters since the removal efficiency of ASB/N,S-TiO$_2$ is higher than RSB/N,S-TiO$_2$ and CSB/N,S-TiO$_2$ in comparison with N,S-TiO$_2$.

Figure 5. Adsorption reaction and photocatalytic degradation of CIP of N,S-TiO$_2$ and three composite materials(condition: pH = 5.5–6, [CIP]$_0$ = 30 ppm, dosage = 0.05 mg).

3.2.2. Effect of pH

The influence of pH in the range 3–11 was studied by performing experiments on the removal of CIP in this pH range; the results are shown in Figure 6. The trend of the CIP concentration as a function of pH was similar for both materials, decreasing more in acidic solutions than in basic solutions. The highest treatment efficiency was observed at a pH in the range of 5.5 to 6 for N,S-TiO$_2$ (78.68%) and ASB/N,S-TiO$_2$ (85.59%). This can be explained by two effects: (i) the surface of sugarcane bagasse after calcination usually carries a negative charge surface when the pH is below 7, which gives CIP a positive charge (the presence of N$^+$) leading to a higher CIP adsorption capacity than in the alkaline environment; (ii) the photocatalytic reaction is also enhanced in acidic solutions due to the increase of reactive oxygen species, specifically the OH$^•$ radicals. This result also agrees with the study of Alireza et al. [11]. Therefore, the pH = 5.5–6 of the CIP solution was applied for further experiments.
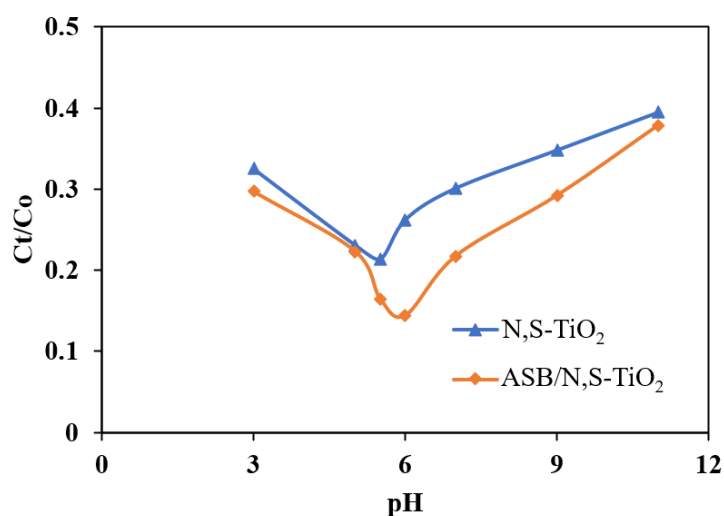
Figure 6. Effect of pH on removal for N,S-TiO$_2$ and ASB/N,S-TiO$_2$ composites (condition: contact time = 150 min irradiation, [CIP]$_0$ = 30 ppm, dosage = 0.05 mg).

3.2.3. Effect of Dosage

The effect of the dosage (0.1–3.5 g/L) of the N,S-TiO$_2$ and ASB/N,S-TiO$_2$ composites was studied. From Figure 7, CIP concentration decreased sharply with an increasing dosage from 0.1 to 1 g/L and gradually declined from 2 to 3.5 g/L for both materials. This may be explained by the increase in the total surface area or the number of active sites. Due to the synergistic interaction between the adsorption and photocatalytic effects of composite materials, ASB/N,S-TiO$_2$ has a higher efficiency than N,S-TiO$_2$. However, an increased material dosage does not yield a proportional increase in removal. Increasing the dosage of the catalyst will generate more oxidizing radicals and improve the efficiency of antibiotic degradation, but an excessive dosage will interfere with the light exposure of N,S-TiO$_2$ photocatalyst. An optimum material weight of 0.5 g L^{-1} was selected for the subsequent experiments.
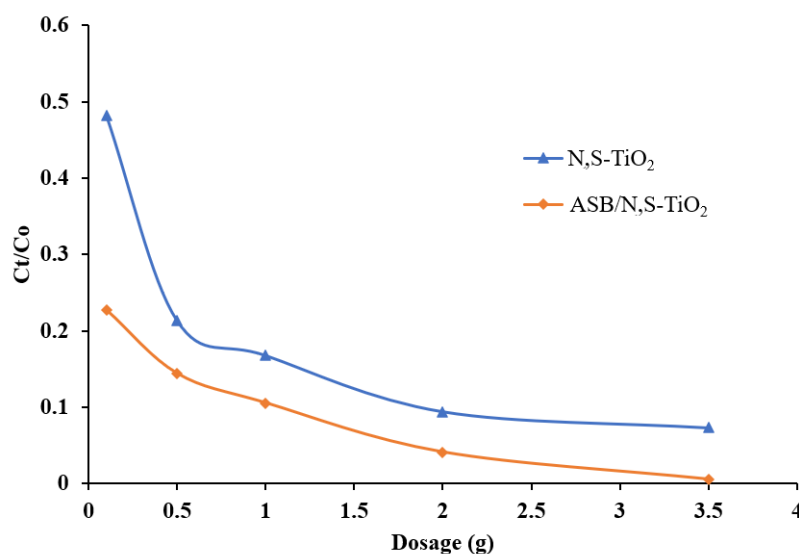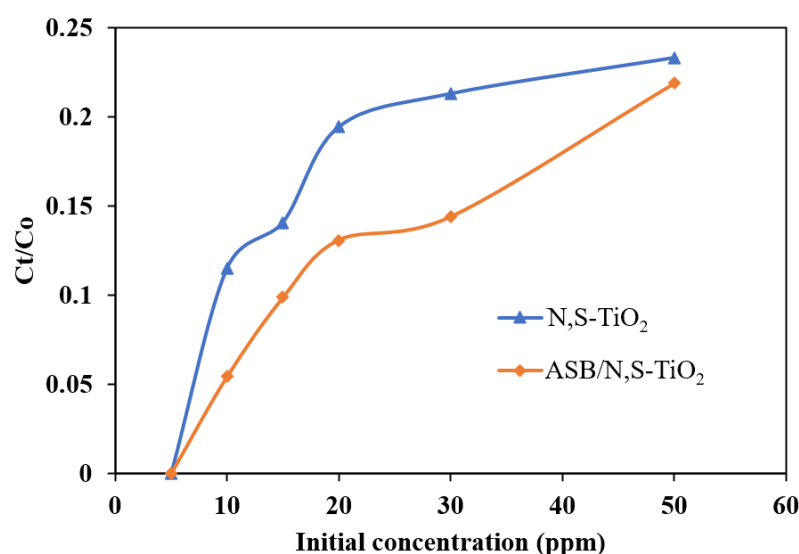

Figure 7. Effect of dosage on removal for N,S-TiO$_2$ and ASB/N,S-TiO$_2$ composites (condition: contact time = 150 min irradiation, [CIP]$_0$ = 30 ppm, pH = 5.5–6).

3.2.4. Effect of Initial Concentration

The effect of the initial concentration of CIP on the performance of N,S-TiO$_2$ and ASB/N,S-TiO$_2$ under UV-vis light by varying its concentration from 5–50 ppm is shown in Figure 8. The efficiency of the two materials in degrading the antibiotic decreased with an increasing initial concentration of CIP. Under a specific dosage and contact time, only a sustained amount of the reactive oxygen species radicals generated will participate in the reaction with the antibiotic molecules. The probability of the reactive oxygen species radicals to reach the antibiotic molecule increases at low concentrations, resulting in high removal efficiency. At higher concentrations, this amount of reactive oxygen species may be less than that of the antibiotic molecules to be eliminated, or exposure to many intermediate products or high antibiotic concentrations that prevent the catalytic material from being exposed to light. The C$_t$/C$_0$ ratio is almost zero at CIP 5 ppm and ranges from 0.11–0.23 for N,S-TiO$_2$ and 0.05–0.21 for ASB/N,S-TiO$_2$ in the C$_0$ range of 10–50 ppm. The ASB/N,S-TiO$_2$ composite always showed better antibiotic treatment than N,S-TiO$_2$ at any initial CIP concentration. Therefore, it can be deduced that alkaline pre-treatment of sugarcane bagasse before binding with N,S-TiO$_2$ is the best pretreatment method to prepare a high-performance hybrid sugarcane bagasse/N,S-TiO$_2$ hybrid photocatalyst in comparison with the other two pre-treatment methods. Depending on the nature of the support material and the photocatalyst different pretreatment methods will bring optimal efficiency. For example, in the study by Xu et al., kaolin that was pre-treated with acid before being combined with TiO$_2$ produced the highest efficiency [22].

Figure 8. Effect of initial concentration on removal for N,S-TiO$_2$ and ASB/N,S-TiO$_2$ composites (condition: contact time = 150 min irradiation, pH = 5.5–6, dosage = 0.05 mg).

3.3. Reusability of ASB/N,S-TiO$_2$ Composite

To assess the long-term performance of the ASB/N,S-TiO$_2$ composite photocatalyst, three consecutive runs were conducted under the same reaction conditions, as shown in Figure 9. The change in the removal efficiency of ASB/N,S-TiO$_2$ in the presence of 30 ppm CIP antibiotic was found to be minimal, with only ~10% (reduced from 85.59% to 77.67%) of treatment activity lost after the third run. The results revealed that the composite photocatalytic activity of ASB/N,S-TiO$_2$ remained relatively stable. This suggests its suitability for water treatment applications.
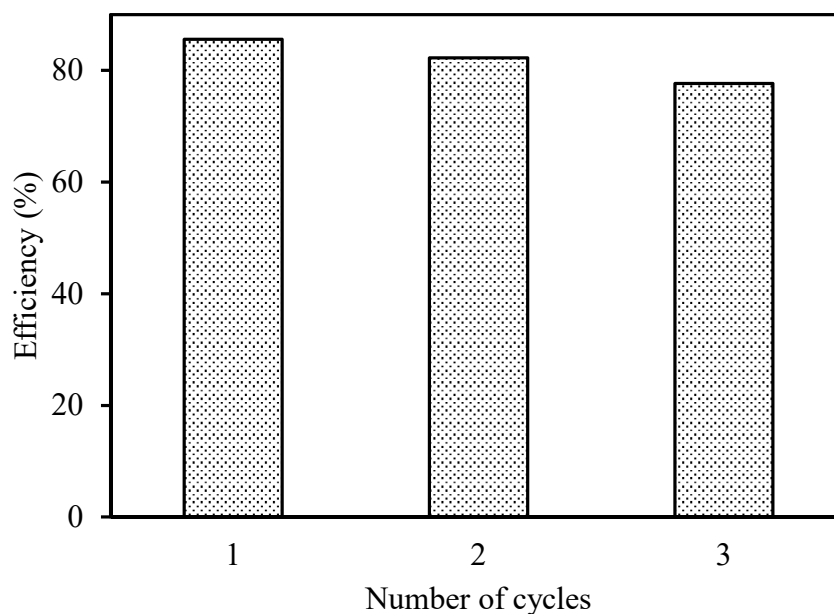
Figure 9. Reusable performance of ASB/N,S-TiO$_2$ composite.

4. Conclusions

Sugarcane bagasse-supported N,S-TiO$_2$ was prepared using a simple sol–gel method that did not change the crystal phase of N,S-TiO$_2$. Among the pre-treatment methods, alkaline pretreatment for sugarcane bagasse had the highest efficiency with a combined adsorption and photocatalysis effect. Sugarcane bagasse in ASB/N,S-TiO$_2$ played a vital

role in the adsorption of antibiotic molecules on the photocatalyst and prevented the recombination of the electron (e^-)/hole (h^+) pair, resulting in the enhanced removal efficiency of CIP antibiotic in comparison with N,S-TiO$_2$. The optimal removal efficiency of ASB/N,S-TiO$_2$ was about 86% at pH = 5.5–6, the weight of the material was 0.05 mg in 100 mL of CIP 30 ppm, adsorption in the dark for 45 min, and exposure to UV-vis light in 150 min. On the other hand, the presence of sugarcane bagasse in ASB/N,S-TiO$_2$ makes the hybrid material easier to diffuse in solution and torecover the photocatalyst after filtration.

References

1. Kosar Hashemi, Y.; Tavakkoli Yaraki, M.; Ghanbari, S.; Heidarpoor Saremi, L.; Givianrad, M.H. Photodegradation of organic water pollutants under visible light using anatase F, N co-doped TiO$_2$/SiO$_2$ nanocomposite: Semi-pilot plant experiment and density functional theory calculations. *Chemosphere* **2021**, *275*, 129903. [CrossRef] [PubMed]
2. Feng, Y.; Dionysiou, D.D.; Wu, Y.; Zhou, H.; Xue, L.; He, S.; Yang, L. Adsorption of dyestuff from aqueous solutions through oxalic acid-modified swede rape straw: Adsorption process and disposal methodology of depleted bioadsorbents. *Bioresour. Technol.* **2013**, *138*, 191–197. [CrossRef] [PubMed]
3. Homem, V.; Santos, L. Degradation and removal methods of antibiotics from aqueous matrices—A review. *J. Environ. Manag.* **2011**, *92*, 2304–2347. [CrossRef] [PubMed]
4. Yang, T.; Yu, D.; Wang, D.; Yang, T.; Li, Z.; Wu, M.; Petru, M.; Crittenden, J. Accelerating Fe(III)/Fe(II) cycle via Fe(II) substitution for enhancing Fenton-like performance of Fe-MOFs. *Appl. Catal. B Environ.* **2021**, *286*, 119859. [CrossRef]
5. Yu, D.; Wang, L.; Yang, T.; Yang, G.; Wang, D.; Ni, H.; Wu, M. Tuning Lewis acidity of iron-based metal-organic frameworks for enhanced catalytic ozonation. *Chem. Eng. J.* **2021**, *404*, 127075. [CrossRef]
6. Yu, D.; Li, L.; Wu, M.; Crittenden, J.C. Enhanced photocatalytic ozonation of organic pollutants using an iron-based metal-organic framework. *Appl. Catal. B Environ.* **2019**, *251*, 66–75. [CrossRef]
7. Hamadanian, M.; Rostami, M.; Jabbari, V. Graphene-supported C–N–S tridoped TiO$_2$ photo-catalyst with improved band gap and charge transfer properties. *J. Mater. Sci. Mater. Electron.* **2017**, *28*, 15637–15646. [CrossRef]
8. García-Muñoz, P.; Carbajo, J.; Faraldos, M.; Bahamonde, A. Photocatalytic degradation of phenol and isoproturon: Effect of adding an activated carbon to titania catalyst. *J. Photochem. Photobiol. A Chem.* **2014**, *287*, 8–18. [CrossRef]
9. Janus, M.; Szyma, K. C-, N- and S-Doped TiO$_2$ Photocatalysts: A Review. *Catalysts* **2021**, *11*, 144.
10. Greenstein, K.E.; Nagorzanski, M.R.; Kelsay, B.; Verdugo, E.M.; Myung, N.V.; Parkin, G.F.; Cwiertny, D.M. Carbon-titanium dioxide (C/TiO$_2$) nanofiber composites for chemical oxidation of emerging organic contaminants in reactive filtration applications. *Environ. Sci. Nano* **2021**, *8*, 711–722. [CrossRef]
11. Khedr, T.M.; El-Sheikh, S.M.; Hakki, A.; Ismail, A.A.; Badawy, W.A.; Bahnemann, D.W. Highly active non-metals doped mixed-phase TiO$_2$ for photocatalytic oxidation of ibuprofen under visible light. *J. Photochem. Photobiol. A Chem.* **2017**, *346*, 530–540. [CrossRef]
12. Jiang, H.; Wang, Q.; Zang, S.; Li, J.; Wang, Q. Enhanced photoactivity of Sm, N, P-tridoped anatase-TiO$_2$ nano-photocatalyst for 4-chlorophenol degradation under sunlight irradiation. *J. Hazard. Mater.* **2013**, *261*, 44–54. [CrossRef] [PubMed]
13. Yao, L.; Wang, H.; Zhang, Y.; Wang, S.; Liu, X. Fabrication of N doped TiO$_2$/C nanocomposites with hierarchical porous structure and high photocatalytic activity. *Microporous Mesoporous Mater.* **2019**, *288*, 109604. [CrossRef]
14. Praneeth, N.V.S.; Paria, S. Clay-supported anisotropic Au-modified N,S-doped TiO$_2$ nanoparticles for enhanced photocatalytic dye degradation and esterification reactions. *New J. Chem.* **2020**, *44*, 2619–2629. [CrossRef]

15. Surenjan, A.; Sambandam, B.; Pradeep, T.; Philip, L. Synthesis, characterization and performance of visible light active C-TiO$_2$ for pharmaceutical photodegradation. *Biochem. Pharmacol.* **2017**, *5*, 757–767.

16. Setthaya, N.; Chindaprasirt, P.; Yin, S.; Pimraksa, K. TiO$_2$-zeolite photocatalysts made of metakaolin and rice husk ash for removal of methylene blue dye. *Powder Technol.* **2017**, *313*, 417–426. [CrossRef]

17. Bel Hadjltaief, H.; Omri, A.; Ben Zina, M.; Da Costa, P.; Galvez, M.E. Titanium Dioxide Supported on Different Porous Materials as Photocatalyst for the Degradation of Methyl Green in Wastewaters. *Adv. Mater. Sci. Eng.* **2015**, *2015*, 759853. [CrossRef]

18. Sayilkan, F.; ASİLTüRK, M.; Şener, Ş.; Erdemoğlu, S.; Erdemoğlu, M.; Sayilkan, H. Hydrothermal synthesis, characterization and photocatalytic activity of nanosized TiO$_2$ based catalysts for rhodamine B degradation. *Turk. J. Chem.* **2007**, *31*, 211–221.

19. Xing, B.; Shi, C.; Zhang, C.; Yi, G.; Chen, L.; Guo, H.; Huang, G.; Cao, J. Preparation of TiO$_2$/Activated Carbon Composites for Photocatalytic Degradation of RhB under UV Light Irradiation. *J. Nanomater.* **2016**, *2016*, 393648. [CrossRef]

20. Khataee, A.; Kayan, B.; Gholami, P.; Kalderis, D.; Akay, S. Sonocatalytic degradation of an anthraquinone dye using TiO2-biochar nanocomposite. *Ultrason. Sonochem.* **2017**, *39*, 120–128. [CrossRef]

21. Kim, J.R.; Kan, E. Heterogeneous photocatalytic degradation of sulfamethoxazole in water using a biochar-supported TiO$_2$ photocatalyst. *J. Environ. Manag.* **2016**, *180*, 94–101. [CrossRef]

22. Xu, H.; Sun, S.; Jiang, S.; Wang, H.; Zhang, R.; Liu, Q. Effect of pretreatment on microstructure and photocatalytic activity of kaolinite/TiO$_2$ composite. *J. Sol-Gel Sci. Technol.* **2018**, *87*, 676–684. [CrossRef]

23. Atout, H.; Alvarez, M.G.; Chebli, D.; Bouguettoucha, A.; Tichit, D.; Llorca, J.; Medina, F. Enhanced photocatalytic degradation of methylene blue: Preparation of TiO$_2$/reduced graphene oxide nanocomposites by direct sol-gel and hydrothermal methods. *Mater. Res. Bull.* **2017**, *95*, 578–587. [CrossRef]

24. Tahir, H.; Sultan, M.; Akhtar, N.; Hameed, U.; Abid, T. Application of natural and modified sugar cane bagasse for the removal of dye from aqueous solution. *J. Saudi Chem. Soc.* **2016**, *20*, S115–S121. [CrossRef]

25. Anukam, A.; Berghel, J. Biomass Pretreatment and Characterization: A Review. *Biomass* **2020**. [CrossRef]

26. Jiang, J.Q.; Zhou, Z.; Pahl, O. Preliminary study of ciprofloxacin (cip) removal by potassium ferrate(VI). *Sep. Purif. Technol.* **2012**, *88*, 95–98. [CrossRef]

27. Roy, N.; Alex, S.A.; Chandrasekaran, N.; Mukherjee, A.; Kannabiran, K. A comprehensive update on antibiotics as an emerging water pollutant and their removal using nano-structured photocatalysts. *J. Environ. Chem. Eng.* **2021**, *9*, 104796. [CrossRef]

28. Rakshit, S.; Sarkar, D.; Elzinga, E.J.; Punamiya, P.; Datta, R. Mechanisms of ciprofloxacin removal by nano-sized magnetite. *J. Hazard. Mater.* **2013**, *246–247*, 221–226. [CrossRef]

29. Tran, N.H.; Reinhard, M.; Gin, K.Y.H. Occurrence and fate of emerging contaminants in municipal wastewater treatment plants from different geographical regions-a review. *Water Res.* **2018**, *133*, 182–207. [CrossRef]

30. Nguyen, L.T.; Nguyen, H.T.; Pham, T.-D.; Tran, T.D.; Chu, H.T.; Dang, H.T.; Nguyen, V.-H.; Nguyen, K.M.; Pham, T.T.; Van Der Bruggen, B. UV–Visible Light Driven Photocatalytic Degradation of Ciprofloxacin by N,S Co-doped TiO$_2$: The Effect of Operational Parameters. *Top. Catal.* **2020**, *63*, 985–995. [CrossRef]

31. Wei, F.; Ni, L.; Cui, P. Preparation and characterization of N-S-codoped TiO$_2$ photocatalyst and its photocatalytic activity. *J. Hazard. Mater.* **2008**, *156*, 135–140. [CrossRef] [PubMed]

32. Mohamed, M.M.; Bayoumy, W.A.; Mansour El-Ashkar, T.Y.; Goher, M.E.; Abdo, M.H. Graphene oxide dispersed in N-TiO$_2$ nanoplatelets and their implication in wastewater remediation under visible light illumination: Photoelectrocatalytic and photocatalytic properties. *J. Environ. Chem. Eng.* **2019**, *7*, 102884. [CrossRef]

33. Kamalakkannan, J.; Chandraboss, V.L.; Prabha, S.; Senthilvelan, S. Activated Carbon Loaded N, S Co-Doped TiO$_2$ Nanomaterial and its Dye Wastewater Treatment. *Int. Lett. Chem. Phys. Astron.* **2015**, *47*, 147–164. [CrossRef]

34. Brindha, A.; Sivakumar, T. Visible active N, S co-doped TiO$_2$/graphene photocatalysts for the degradation of hazardous dyes. *J. Photochem. Photobiol. A Chem.* **2017**, *340*, 146–156. [CrossRef]

35. El-Sheikh, S.M.; Khedr, T.M.; Hakki, A.; Ismail, A.A.; Badawy, W.A.; Bahnemann, D.W. Visible light activated carbon and nitrogen co-doped mesoporous TiO$_2$ as efficient photocatalyst for degradation of ibuprofen. *Sep. Purif. Technol.* **2017**, *173*, 258–268. [CrossRef]

36. Hassani, A.; Khataee, A.; Karaca, S.; Karaca, C.; Gholami, P. Sonocatalytic degradation of ciprofloxacin using synthesized TiO$_2$ nanoparticles on montmorillonite. *Ultrason. Sonochem.* **2017**, *35*, 251–262. [CrossRef]